JPET Fast Forward. Published on January 22, 2019 as DOI: 10.1124/jpet.118.254961
This article has not been copyedited and formatted. The final version may differ from this version.



# 1. Title page

**Title**

Squalene-adenosine nanoparticles: ligands of adenosine receptors or adenosine prodrug?

**Authors**

Marie Rouquette, Sinda Lepetre-Mouelhi, Ophélie Dufrançais, Xue Yang, Julie Mougin, Grégory Pieters, Sébastien Garcia-Argote, Adriaan P. IJzerman and Patrick Couvreur

**Affiliations**

M.R., S. L.-M., O. D., J. M., P. C.: Institut Galien Paris-Sud, Université Paris-Sud, CNRS, Université Paris Saclay, Châtenay-Malabry, France

X. Y., A. P. IJ.: Division of Medicinal Chemistry, Leiden Academic Centre for Drug Research Leiden University, Leiden, the Netherlands

G. P., S. G.-A.: Service de Chimie Bioorganique et de Marquage (SCBM), CEA, Université Paris-Saclay, Gif-sur-Yvette, France

JPET Fast Forward. Published on January 22, 2019 as DOI: 10.1124/jpet.118.254961
This article has not been copyedited and formatted. The final version may differ from this version.



# 2. Running title page

## a) Running title

Squalene-adenosine nanoparticles: ligands or prodrug?

## b) Corresponding author

Patrick Couvreur

UMR CNRS8612
Institut Galien Paris-Sud
Faculté Pharmacie Paris-Sud
5, rue J-B Clément
92290 Châtenay-Malabry
France

Phone: 01 46 83 53 96

Fax: 01 46 61 93 34

patrick.couvreur@u-psud.fr

## c) Numbers

Number of text pages: 29 (excluding figures legends, tables and figures)

Number of tables: 1

Number of figures: 7

Numbers of references: 15

Number of words in the Abstract: 257

Number of words in the Introduction: 462

Number of words in the Discussion: 713

### d) Nonstandard abbreviations

| | |
|---|---|
| [$^3$H]DPCPX | 1,3-[$^3$H]-dipropyl-8-cyclopentylxanthine |
| [$^3$H]PSB11 | [$^3$H]8-Ethyl-4-methyl-2-phenyl-(8R)-4,5,7,8-tetrahydro-1H-imidazo[2,1-i]-purin-5-one |
| [$^3$H]PSB603 | [$^3$H]8-(4-(4-(4-Chlorophenyl)piperazide-1-sulfonyl)phenyl)-1-propylxanthine |
| [$^3$H]ZM241385 | [2-$^3$H]-4-(2-[7-amino-2-{2-furyl}{1,2,4}triazolo{2,3-a}{1,3,5,}triazin-5-yl amino]ethyl)phenol |
| Ad | Adenosine |
| ADA | Adenosine deaminase |
| AR | Adenosine receptor |
| BCA | Bicinchoninic acid |
| bFGF | Basic fibroblast growth factor |
| CHO | Chinese hamster ovary cells |
| CholEsteryl BODIPY™ FL $C_{12}$ | CholEsteryl 4,4-difluoro-5,7-dimethyl-4-bora-3a,4a-diaza-s-indacene-3-dodecanoate |
| CPA | $N^6$-cyclopentyladenosine |
| DAPI | 4′,6-diamidino-2-phenylindole |
| DLS | Dynamic light scattering |
| DMEM | Dulbecco's Modified Eagle's Medium |
| DMSO | Dimethyl sulfoxide |
| EBM-2 | Endothelial basal medium |
| EHNA | Erythro-9-(2-hydroxy-3-nonyl)-adenine |
| ENT | Equilibrative nucleoside transporter |

| | |
|---|---|
| FBS | Fetal bovine serum |
| GPCR | G protein-coupled receptor |
| HPLC | High-performance liquid chromatography |
| IBMX | Isobutyl-1-methylxanthine |
| Ki | Ligand binding affinity |
| LDL | Low-density lipoprotein |
| LDLR | Low-density lipoproteins receptor |
| LPDS | Lipoprotein deficient serum |
| NECA | 5'-N-ethylcarboxamidoadenosine |
| NP | Nanoparticle |
| NSB | Non-specific binding |
| PBS | Dulbecco's phosphate buffered saline |
| PdI | Polydispersity index |
| pKi | - Log(Ki) |
| RLU | Relative Luminescence Unit |
| Ro 20-1724 | 4-(3-butoxy-4-methoxybenzyl) imidazolidone |
| SQAd | Squalene-adenosine |
| TB | Total binding |
| WGA | Wheat germ agglutinin |
| ZM241385 | 4-(-2-[7-amino-2-{2-furyl}{1,2,4}triazolo{2,3-a}{1,3,5}triazin-5-yl-amino]ethyl)phenol |

**e) Recommended section**

Drug Discovery and Translational Medicine

## 3. Abstract

Adenosine receptors (ARs) represent key drug targets in many human pathologies, including cardiovascular, neurological and inflammatory diseases. To overcome the very rapid metabolization of adenosine, metabolically stable ARs agonists and antagonists were developed. However, few of these molecules have reached the market due to efficacy and safety issues. Conjugation of adenosine to squalene to form squalene-adenosine nanoparticles (SQAd NPs) dramatically improved the pharmacological efficacy of adenosine, especially for neuroprotection in stroke and spinal cord injury. However, the mechanism by which SQAd NPs displayed therapeutic activity remained totally unknown. In the present study, two hypotheses were discussed: (i) either SQAd bioconjugates, which constitute the NPs building blocks, act directly as ARs ligands, or (ii) adenosine, once released from intracellularly processed SQAd NPs, interacts with these receptors. The first hypothesis was rejected, using radioligand displacement assays, as no binding to human ARs was detected up to 1 µM of SQAd, in the presence of plasma. Hence, the second hypothesis was examined. SQAd NPs uptake by HepG2 cells, which was followed using radioactive and fluorescence tagging, was found to be independent of equilibrative nucleoside transporters but rather mediated by low-density lipoproteins receptors. Interestingly, it was observed that after cell internalization, SQAd NPs operated as an intracellular reservoir of adenosine, followed by a sustained release of the nucleoside in the extracellular medium. This resulted in a final paracrine-like activation of ARs pathway, evidenced by fluctuations of the second messenger cAMP. This deeper understanding of SQAd NPs mechanism of action provides now strong rational for extending the pharmaceutical use of this nanoformulation.

## 4. Introduction

Adenosine is an endogenous purine acting on four different G protein-coupled receptors (GPCRs) identified as $A_1$, $A_{2A}$, $A_{2B}$ and $A_3$. The wide distribution of these adenosine receptors (ARs) is associated with a great diversity of pathophysiological effects, including regulation of cardiovascular, nervous and immune systems (Fredholm et al., 2011). Although considerable efforts have been devoted to identifying new compounds interacting with ARs (Borea et al., 2018), very few molecules have reached the clinic due to activity and/or toxicity issues. On the other hand, because of a very short half-life in the blood circulation ($t_{1/2} \sim 10$ s), adenosine must be administered at high doses which results in severe side effects, thus limiting the clinical use of this molecule. Therefore, innovative pharmaceutical strategies are still needed to fully exploit adenosine's tremendous therapeutic potential.

Currently, the so-called "squalenoylation" approach may represent a promising technological platform for delivering hydrophilic compounds with stability issues or off-target toxicity (Couvreur et al., 2006). This methodology consists of the conjugation of a fragile and quickly metabolized drug molecule to the squalene, a natural and biocompatible lipid. Interestingly, the resulting drug-squalene bioconjugates have the unique ability to self-assemble in water as nanoparticles (NPs). It was found that these squalene-based NPs favorably modified the *in vivo* pharmacokinetics and biodistribution of the conjugated drug molecules (Reddy et al., 2007). In particular, the delivery of adenosine via squalene-adenosine (SQAd) NPs showed an impressive neuroprotective efficacy in brain ischemia in mice and in spinal cord injury in rats (Gaudin et al., 2014). This effect was explained by a prolonged circulation of SQAd NPs into the bloodstream compared to free adenosine (Gaudin et al., 2015), and appeared to originate from the interaction of

SQAd NPs with the brain endothelial cells. However, the nature of the interaction between SQAd NPs and cells still remains totally unknown.

Thus, the current study aims at elucidating the mechanism of action of SQAd NPs *in vitro*. Two hypotheses were tested: (i) either the SQAd NPs or SQAd bioconjugates would act as direct ARs agonists (or antagonists) by binding them via their adenosine moiety; or (ii) they would function as prodrugs, by slowly releasing adenosine intracellularly and into the extracellular space.

The first hypothesis was checked by radioligand displacement assays on membrane fractions of cells overexpressing human ARs. The second hypothesis was tested on the HepG2 cell line, a well-characterized *in vitro* human hepatocyte model. Liver cells were chosen for this study as it has previously been shown that SQAd NPs accumulate in high quantities in the liver after their intravenous injection in mice (Gaudin et al., 2015). The cell capture of SQAd NPs was followed by radiolabeling and fluorescent labeling, while adenosine release was determined by high-performance liquid chromatography (HPLC). Finally, the activation of the adenosine receptors was also evaluated.

JPET Fast Forward. Published on January 22, 2019 as DOI: 10.1124/jpet.118.254961
This article has not been copyedited and formatted. The final version may differ from this version.



## 5. Materials and methods

### *5.1. Materials*

SQAd bioconjugate originated from Holochem (Val-de-Reuil, France). D-(+)-glucose was obtained from Sigma (St Quentin Fallavier, France). Absolute ethanol and methanol came from VWR Chemicals (Strasbourg, France) while dimethyl sulfoxide was from Carlo Erba Reagents (Val-de-Reuil, France). MilliQ® water (resistivity 18.2 MΩ·cm) was purified on a system from Millipore (Molsheim, France). CholEsteryl 4,4-Difluoro-5,7-Dimethyl-4-Bora-3a,4a-Diaza-s-Indacene-3-Dodecanoate (CholEsteryl BODIPY™ FL $C_{12}$) and wheat germ agglutinin (WGA) Alexa Fluor$^{TM}$ 555 conjugate were purchased from ThermoFisher Scientific (Karlsruhe, Germany). [2,8-$^{3}$H]-Adenosine (specific activity 20.3 Ci/mmol) was obtained from Moravek Biochemicals (Brea, CA, USA) while SQ-[$^{3}$H]-Ad (specific activity 2.8 Ci/mmol) was synthetized as previously reported (Gaudin et al., 2014). Soluene-350 and Hionic Fluor were provided by Perkin Elmer (Courtaboeuf, France). Radioligands 1,3-[$^{3}$H]-dipropyl-8-cyclopentylxanthine ([$^{3}$H]DPCPX, specific activity of 120 Ci/mmol) and [2-3H]-4-(2-[7-amino-2-{2-furyl}{1,2,4}triazolo{2,3-a}{1,3,5,}triazin-5-yl amino]ethyl)phenol ([$^{3}$H]ZM241385, specific activity of 50 Ci/mmol) were purchased from ARC Inc. (St.Louis, MO). [$^{3}$H]8-(4-(4-(4-Chlorophenyl)piperazide-1-sulfonyl)phenyl)-1-propylxanthine ([$^{3}$H]PSB603**,** specific activity 79 Ci/mmol) and [$^{3}$H]8-Ethyl-4-methyl-2-phenyl-(8R)-4,5,7,8-tetrahydro-1H-imidazo[2,1-i]-purin-5-one ([$^{3}$H]PSB11, specific activity 56 Ci/mmol) were kindly provided by Prof. C.E. Müller (University of Bonn, Germany). 5'-N-ethylcarboxamidoadenosine (NECA) was purchased from Sigma-Aldrich (Steinheim, Germany). N$^{6}$-cyclopentyladenosine (CPA) was purchased from Abcam (Cambridge, UK). Unlabelled ZM241385 was a gift from Dr. S.M.Poucher (Astra Zeneca, Macclesfield, UK). Adenosine deaminase (ADA) was purchased from Boehringer Mannheim (Mannheim, Germany).

JPET Fast Forward. Published on January 22, 2019 as DOI: 10.1124/jpet.118.254961
This article has not been copyedited and formatted. The final version may differ from this version.



Bicinchoninic acid (BCA) and BCA protein assay reagent were obtained from Pierce Chemical Company (Rockford, IL, USA). Chinese hamster ovary cells stably expressing the human adenosine $A_1$ receptor (CHOh$A_1$AR), $A_{2B}$ (CHOh$A_{2B}$AR) and $A_3$ receptor (CHOh$A_3$AR) were provided by Prof. S. J. Hill (University of Nottingham, UK), Dr. S. Rees (AstraZeneca, Macclesfield, UK) and Dr. K-N. Klotz (University of Würzburg, Germany), respectively. HEK293 cells stably expressing the h$A_{2A}$ adenosine receptor (HEK293 h$A_{2A}$AR) were kindly provided by Dr J Wang (Biogen/IDEC, Cambridge, MA, USA). hCMEC/D3 cell line was a gift from Pr. Couraud (Hôpital Cochin, Paris, France). HepG2 cell line, Dulbecco's Modified Eagle's Medium (DMEM) high glucose, Dulbecco's phosphate buffered saline (PBS), lipoprotein deficient serum (LPDS) from fetal calf, trypsin and penicillin-streptomycin, HEPES, hydrocortisone, basic fibroblast growth factor (bFGF), ascorbic acid, adenosine, cathepsin B from human liver, theophylline, dipyridamole, erythro-9-(2-hydroxy-3-nonyl)-adenine (EHNA) hydrochloride, paraformaldehyde, isobutyl-1-methylxanthine (IBMX) and 4-(3-butoxy-4-methoxybenzyl) imidazolidone (Ro 20-1724) were obtained from Sigma (St Quentin Fallavier, France). Endothelial Basal Medium (EBM-2) medium was purchased from Lonza (Basel, Switzerland). Gibco™ fetal bovine serum (FBS) was obtained from Life Technologies (Saint-Aubin, France).

All other chemicals were of analytical grade and obtained from standard commercial sources.

*5.2. SQAd NPs preparation*

SQAd NPs were prepared as previously described (Gaudin et al., 2014). Briefly, 333 µL of an ethanolic solution of 6 mg/mL SQAd was added dropwise into 1 mL of a solution of 5 wt. % dextrose under stirring. Ethanol was then removed by evaporation using a Rotavapor to obtain a final concentration of 2 mg/mL SQAd NPs. Radiolabeled NPs were obtained following the same

JPET Fast Forward. Published on January 22, 2019 as DOI: 10.1124/jpet.118.254961
This article has not been copyedited and formatted. The final version may differ from this version.



procedure, with the addition of [$^3$H]-SQAd to the ethanolic SQAd solution (final radioactivity 10 Ci/mol). Similarly, fluorescently labeled SQAd NPs were prepared by adding 40 µL CholEsteryl BODIPY FL $C_{12}$ to the 333 µL ethanolic SQAd solution (the final concentration of fluorescent probe was 1 wt. %). Excitation and emission spectra were recorded using a LS 50B Luminescence Spectrometer (Perkin Elmer) (**Supplementary Figure 1**).

The mean NPs size and polydispersity index (PdI) were checked from 1 mg/mL suspensions by dynamic light scattering (DLS) using a Zetasizer Nano ZS (173° scattering angle, 25 °C) (Malvern, UK).

*5.3. Radioligand displacement assay*

CHOh$A_1$A, CHOh$A_{2B}$AR, CHOh$A_3$AR and HEK293 h$A_{2A}$AR cells were cultured and membranes were prepared as previously described (Heitman et al., 2009; Yang et al., 2017). Buffers compositions, membranes concentrations, radioligands and non-specific binding compounds used for each receptor type, as well as their concentrations, are listed in **Supplementary Table 1**.

For radioligand displacement assays, membrane aliquots at given concentrations (**Supplementary Table 1**) were incubated in a total volume of 100 µL assay buffer (**Supplementary Table 1**) at 25 °C for 60 min ($A_1$) to 120 min (other receptors). The dimethyl sulfoxide (DMSO) stock solution of SQAd as single bioconjugate molecules and the SQAd NPs preparation were diluted in assay buffer or FBS (DMSO final concentration < 1 %). Samples with serum were incubated for 4 h at 37 °C on a Thermoshaker before the experiment. Displacement experiments were performed in the presence of specific radioligands at given concentrations (**Supplementary Table 1**), while nonspecific binding was determined in the presence of non-specific binding compounds at given concentrations (**Supplementary Table 1**). Incubations were terminated by dilution with ice-cold assay buffer, immediately followed by separation of bound

from free radioligand by rapid filtration through 96-well GF/B filter plates using a Perkin Elmer Filtermate-harvester (PerkinElmer, Groningen, Netherlands). Filters were subsequently washed three times with 2 mL of ice-cold washing buffer (**Supplementary Table 1**). The filter-bound radioactivity was determined by scintillation spectrometry using a P-E 1450 Microbeta Wallac Trilux scintillation counter (PerkinElmer). $IC_{50}$ values were obtained by fitting the curves with a one-site binding model using GraphPad Prism 7.00 software. Ki values were deduced using the Cheng-Prusoff equation (Cheng and Prusoff, 1973).

*5.4. Cell culture*

HepG2 cells were cultured in DMEM high glucose medium supplemented with 10 % FBS, penicillin (50 U/mL) and streptomycin (50 µg/mL). If not stated otherwise, cells were plated on 24-well plates at a density of 200 000 cells per well and left to adhere overnight before any further procedure.

hCMEC/D3 cells were cultured in EBM-2 medium supplemented with 5% FBS, penicillin (50 U/mL) and streptomycin (50 µg/mL), 1.4 µM hydrocortisone, 5 µg/mL acid ascorbic, 1% Chemically Defined Lipid Concentrate, 10 mM HEPES and 1 ng/mL bFGF. Cells were used between passages 4 and 8. Cells were plated on 24-well plates at a density of 100 000 cells per well and left to adhere overnight before any further procedure.

All cells were maintained at 37 °C, 5 % $CO_2$, 100 % humidity. Cells were passaged twice a week.

*5.5. Cell uptake of radiolabeled SQAd NPs and free adenosine*

HepG2 cells were treated with radiolabeled SQAd NPs or radiolabeled free adenosine at a concentration of 10 µM and 0.1 µCi/mL. At different time points, cells were washed twice with

PBS and detached with trypsin before been pelleted and resuspended in PBS. Samples radioactivity was measured using a β-scintillation counter (Beckman Coulter LS6500) after overnight incubation with 1 mL Soluene-350 at 50 °C and addition of 10 mL Hionic Fluor.

*5.6. Cell uptake of fluorescently labeled SQAd NPs*

For confocal microscopy imaging, HepG2 cells were plated onto sterile glass coverslips placed in 24-well plates, at a density of 50 000 cells per well, and left to adhere for 48 h. Cells were incubated with fluorescently labeled SQAd NPs (10 µg/mL) for 2 h at 37 °C. After several washing steps with PBS, membranes were stained for 20 min with 10 µg/mL of WGA Alexa Fluor 555. Cells were then washed again and fixed with 4 % paraformaldehyde for 15 min. After final washing, coverslips were mounted on slides using Vectashield® mounting medium with 4′,6-diamidino-2-phenylindole (DAPI) and sealed with nail polish. Images were acquired using a Leica TCS SP8 system, with a Plan Apochromat 63×/1.4NO oil objective lens.

For studying the role of adenosine transporters, HepG2 cells were treated with fluorescently labeled SQAd NPs (10 µg/mL) and dipyridamole (20 µM). For studying the role of low-density lipoproteins receptors (LDLRs) in SQAd NPs cell uptake, 150 000 cells were plated by well. Cells were washed with PBS and medium was replaced with normal medium or medium supplemented with LPDS instead of FBS. Cells were then incubated for 24 h to enhance LDLRs expression, as proven by Western Blot (protocol from (Sobot et al., 2017a), **Supplementary Figure 2**) and subsequently treated with fluorescently labelled SQAd NPs (10 µg/mL). In both cases, after 30 min or 2 h, cells were finally washed with PBS, detached with trypsin and resuspended in PBS. Cell fluorescence was evaluated using a BD Accuri™ C6 flow cytometer (BD Biosciences) with an excitation wavelength of 488 nm. Emission was recorded with the FL1 filter (533/30 nm).

*5.7. SQAd degradation in acidic conditions*

A solution of 1 µL SQAd (2.5 mg/mL dissolved in DMSO) was incubated at 37 °C under shaking in 100 µL of 0.3 M pH 4.8 sodium acetate buffer containing cathepsin B (10 U/mL). Degradation was stopped at different time points by the addition of 233 µL methanol. 5 µL gemcitabine-squalene (0.2 mg/mL dissolved in DMSO) were added as internal standard. Samples were centrifuged (14 000 rpm, 10 min) and resulting supernatants were evaporated to dryness at 37 °C under air flow. The dried samples were then dissolved in 100 µL of mobile phase (methanol for SQAd detection; methanol/$KH_2PO_4$ (10 mM, pH 4) 20/80 v/v, for adenosine detection) prior to HPLC analysis.

*5.8. Adenosine extracellular release*

HepG2 or hCMEC/D3 cells were treated with SQAd NPs (100 µM), free adenosine dissolved in 5 wt. % dextrose (100 µM) or 5 wt. % dextrose. After 5 min to 4 h, extracellular medium was replaced by 1 mL of simplified medium (composition is given in **Supplementary Table 2**) supplemented with 50 µM EHNA (to avoid adenosine deamination) and 2 µM internal standard (theophylline). After 5 min to 4 h, the extracellular medium was collected and extracted with 2.3 mL of methanol. Samples were centrifuged at 17 000 x *g* for 10 min to remove insoluble materials and supernatants were filtered and evaporated to dryness at 37 °C under air flow. The dried samples were dissolved in 100 µL of mobile phase (methanol/$KH_2PO_4$ (10 mM pH 4) 20/80 v/v) and filtered before HPLC analysis. The detection limit of the HPLC technique was 17 nM for the adenosine, while the quantification limit was 55 nM. This method exhibited linearity ($R^2$ = 0.99) over the assayed concentration range (100 - 1000 nM) and demonstrated good precision with relative standard deviation (RSD) being all less than 5%.

*5.9. HPLC conditions*

A Water™ 717 plus autosampler was employed equipped with a Waters™ 1525 binary HPLC pump, a Waters™ 2487 dual λ absorbance detector, and a Waters™ Breeze software. The analysis was performed using a Halo C18 column (4.6 x 250 mm, 5 µm; Interchim, France). The injection volume was 40 µL to 50 µL, the elution was carried out at 0.8 mL/min isocratically for 10 min with the column temperature maintained at 30 °C. Detection wavelengths were respectively 273 nm for SQAd and 260 nm for adenosine.

*5.10. Intracellular cAMP levels*

The day before the experiment, two plates were seeded with HepG2 cells: a 24-well plate with 200 000 cells per well and a 96-well plate with 5 000 cells per well.

On the day of the experiment, cells in the 24-well plate were treated with SQAd NPs, free adenosine or dextrose as previously described. After 2 h, extracellular medium was replaced with simplified medium containing 50 µM EHNA and broad-range phosphatase inhibitors (500 µM IBMX and 100 µM Ro 20-1724). After 1 h, 10 µL of this extracellular medium was used to stimulate cells plated in the 96-well plate for 15 min. cAMP intracellular levels were then determined using the cAMP-Glo™ assay from Promega. Briefly, cells were lysed with 10 µL cAMP-Glo™ Lysis Buffer for 15 min with shaking at room temperature. cAMP-Glo™ Detection Solution and Kinase-Glo Reagent were then added to all wells according to the manufacturer's protocol. Luminescence was detected using an EnSpire Alpha 2390 plate reader (Perkin-Elmer, USA).

JPET Fast Forward. Published on January 22, 2019 as DOI: 10.1124/jpet.118.254961
This article has not been copyedited and formatted. The final version may differ from this version.



## 6. Results

### *6.1. SQAd NPs*

Prepared by nanoprecipitation, SQAd NPs suspensions were monodisperse, displaying a hydrodynamic diameter of 71 ± 15 nm, a PdI of 0.08 ± 0.02 and a drug loading of 37%.

### *6.2. SQAd interaction with human adenosine receptors*

The direct interaction of SQAd with human ARs was checked by radioligand displacement assays. Specific radioligands were used for each adenosine receptor and their displacement was measured in the presence of increasing concentrations of SQAd bioconjugate or NPs. Results are shown in **Figure 1**.

Up to 1 µM, SQAd showed no interaction with any of the ARs in the assay buffer, whether as a bioconjugate or assembled as NPs (**Figure 1A** and **Figure 1B** respectively). At and above 10 µM, some displacement became detectable, with both SQAd bioconjugates and NPs showing a slight preference for the adenosine $A_3$ receptor (**Figure 1A** and **Figure 1B**). Using the Cheng-Prusoff equation, the magnitude of SQAd (bioconjugate or NPs) affinity for each of these receptors was determined. Results are given in **Table 1**. All ligand binding affinities (Ki) were in the micromolar to the millimolar range.

To be as close as possible to the *in vitro* and *in vivo* conditions, SQAd bioconjugates and SQAd NPs were also preincubated for 4 h at 37 °C with FBS, prior to performing the radioligand displacement assay. It should be noted that the interaction with adenosine $A_{2B}$ receptor could not be evaluated under these conditions, due to unspecific interactions between the membranes and the FBS. Regarding the three other receptors, no interaction with SQAd bioconjugate or NPs could be detected anymore, even at the highest concentration (**Figure 1C** and **Figure 1D**). Hence, it was

JPET Fast Forward. Published on January 22, 2019 as DOI: 10.1124/jpet.118.254961
This article has not been copyedited and formatted. The final version may differ from this version.



concluded that the preincubation with serum prevented interaction of SQAd with adenosine receptors.

*6.3. SQAd NPs internalization*

To follow the cell uptake of SQAd NPs, radiolabeled NPs were prepared by co-nanoprecipitation of SQAd and [$^3$H]-SQAd (for more information, see Materials and Methods section), with no influence of the radiolabeled compound on the NPs hydrodynamic diameter (56 ± 4 nm) or PdI (0.10 ± 0.04). HepG2 cells were then incubated at 37 °C for different times with either radiolabeled SQAd NPs or [$^3$H]-adenosine. The resulting intracellular radioactivity is presented in **Figure 2**.

Both adenosine and SQAd NPs were internalized by HepG2 cells. However, the cell uptake of SQAd NPs occurred slower and to a lower extend than free adenosine. Indeed, after 30 min incubation, the intracellular content in adenosine (and its tritiated metabolites) was 13-times higher than with SQAd (and its metabolites). After 24 h, however, the adenosine over SQAd ratio was reduced to a value of only 3.

For further experiments, fluorescently labeled SQAd NPs (diameter of 60.8 ± 0.4 nm, PdI of 0.13 ± 0.01) were prepared by co-nanoprecipitation of SQAd with a fluorescent BODIPY-cholesteryl ester dye. Fluorescent nanoparticles maximum excitation and emission wavelengths were respectively of 484 nm and 520 nm (**Supplementary Figure 1**). NPs uptake by HepG2 cells was visualized by confocal microscopy and measured by flow cytometry under various conditions (**Figure 3**). The fluorescently labeled SQAd NPs were found to be taken up by HepG2 cells (2h incubation) (**Figure 3A**), while no fluorescence was visible when the cells were incubated with the fluorescent probe alone (**Figure 3B**). Hence, the intracellular fluorescence was considered to correlate well with SQAd NPs uptake.

Then, considering that adenosine enters the cells via equilibrative nucleoside transporters (ENTs) (Baldwin et al., 2004), the cellular mechanism of uptake of SQAd NPs was also investigated using HepG2 cells treated with dipyridamole, an ENT inhibitor. After 30 min or 2 h of incubation with fluorescently labeled NPs, no difference in intracellular fluorescence was observed between cells pre-incubated with or without dipyridamole (**Figure 3C**), which clearly indicated that SQAd NPs did not enter the cells via ENTs.

The role of LDLRs was then evaluated by tuning their level of expression on HepG2 cells. Cells were preincubated for 24 h with FBS-supplemented medium (containing normal level of lipoproteins), and LPDS-supplemented medium (containing low levels of lipoproteins). Cell starvation using LPDS induced an over-expression of LDLRs, as evident from Western Blot (**Supplementary Figure 2**). Noteworthy, in LPDS-supplemented medium, cells were found to internalize higher levels of fluorescently labeled SQAd NPs (**Figure 3D**), thus demonstrating an influence of LDLRs expression level on SQAd NPs uptake.

*6.4. SQAd degradation in acidic conditions*

Assuming that once in the cell, SQAd would undergo hydrolysis in acidic endo-lysosomal compartments, SQAd degradation was then evaluated over 24 h in acidic conditions (pH 4.8) in the presence or in the absence of cathepsin B, a typical lysosomal enzyme able to cleave amide bonds. The percentage of intact prodrug under these conditions is shown in **Figure 4A**.

Although almost no bioconversion of the SQAd bioconjugate could be observed until 6 h, up to 20 % of SQAd was degraded after 24 h of incubation in acidic conditions. The presence of cathepsin B did not influence the degradation profile over 24 h. Interestingly, the degradation of SQAd led to the release of free adenosine (retention time 3.9 min), which was characterized by HPLC analysis (**Figure 4B**).

JPET Fast Forward. Published on January 22, 2019 as DOI: 10.1124/jpet.118.254961
This article has not been copyedited and formatted. The final version may differ from this version.



Hence, SQAd intracellular bioconversion into adenosine should increase the adenosine intracellular content. And, as a result of the equilibrium between the intracellular and the extracellular adenosine levels, it was hypothesized that some adenosine could be further released in the extracellular compartment.

*6.5. Adenosine extracellular release*

Thus, the concentration of adenosine released in the cell culture medium was then determined by HPLC in the presence of EHNA, an inhibitor of adenosine deaminase. After incubation of HepG2 (or hCMEC/D3) cells with SQAd NPs, free adenosine or 5 % dextrose solution, the extracellular medium was replaced by 1 mL of a new simplified medium (composition is given in **Supplementary Table 2**) to remove adenosine (eventually resulting from the release from SQAd NPs before their capture by the cells). After further 5 min to 4 h incubation, the extracellular medium was finally collected to determine the quantity of adenosine released from the cells after exposure to SQAd NPs or adenosine (**Figure 5A**).

After 5 min incubation, cells treated with free adenosine released higher concentrations of adenosine (around 600 nM) than cells treated with dextrose or SQAd NPs (100 nM to 200 nM). This clearly highlighted the almost instantaneous ability of the cells to uptake free adenosine, while SQAd NPs uptake and cleavage (which results in adenosine metabolite release) required more time (**Figure 5A**). Interestingly, after longer incubation time with free adenosine, a decrease in adenosine release was observed, which likely resulted from a consumption of the overall pool of adenosine by the cells. On the contrary, after longer incubation time with SQAd NPs, higher levels of released adenosine were observed, which correlated well with an increased intracellular content of SQAd over time, hence producing a reservoir effect. Of note, very close results were obtained

JPET Fast Forward. Published on January 22, 2019 as DOI: 10.1124/jpet.118.254961
This article has not been copyedited and formatted. The final version may differ from this version.



with hCMEC/D3 cells, a brain endothelial cell line derived from human temporal lobe microvessels (**Supplementary Figure 3**).

To further study the intracellular reservoir effect of adenosine produced after incubation with SQAd NPs, cells were incubated for 2 h with free adenosine, SQAd NPs or dextrose and the kinetics of adenosine release from the cells into the extracellular medium was determined. Results are shown in **Figure 5B**. Interestingly, concentrations of released adenosine after incubation of the cells with dextrose or free adenosine did not increase over time, thus revealing that a situation of equilibrium was reached from the first minutes post-incubation. On the contrary, when the cells were incubated with SQAd NPs, quantities of adenosine released by the cells increased over time. This clearly confirmed the reservoir effect resulting from the intracellular accumulation of SQAd NPs followed by the progressive cleavage of the SQAd bioconjugate, allowing a progressive release of free adenosine in the extracellular medium.

A remaining question was to know whether the released adenosine in the extracellular medium was capable of interaction with adenosine receptors on neighboring cells.

*6.6. Adenosine receptors activation*

Thus, adenosine receptors activation was evaluated by measuring the levels of intracellular cAMP. Indeed, adenosine receptors are G protein-coupled receptors (GPCR) known to activate or inhibit adenylate cyclase, hence tuning intracellular levels of cAMP. As in the previous set of experiments, HepG2 cells were incubated with dextrose, free adenosine or SQAd NPs for 2 h and then allowed to release adenosine during 1 h in their extracellular medium. This medium was then used as adenosine pool to investigate the interaction, through 15 min incubation, with other naïve cells by measuring their intracellular cAMP levels. As can be seen in **Figure 6**, the extracellular medium originating from cells treated with control vehicle (5 wt. % dextrose) or free adenosine did not

induce major changes in intracellular cAMP levels. However, extracellular medium arising from cells treated with SQAd NPs induced a significant increase in cAMP, comparatively to vehicle. Interestingly, adenosine levels in extracellular medium originating from cells treated with SQAd NPs or free adenosine were very close under the conditions used (2 h of treatment and 1 h of release, cf. **Figure 5A**). Hence, adenosine might not be the only factor in the extracellular medium interacting with GPCRs.

JPET Fast Forward. Published on January 22, 2019 as DOI: 10.1124/jpet.118.254961
This article has not been copyedited and formatted. The final version may differ from this version.



## 7. Discussion

This study aimed at clarifying the mechanism of action of SQAd NPs *in vitro*. The main question was to determine whether SQAd acted directly on ARs as a specific ligand, or indirectly as a prodrug releasing active adenosine.

By using radioligand displacement experiments, it was measured that SQAd as bioconjugate or as NPs displayed a rather weak affinity for human ARs, showing Ki superior to $10^{-6}$ M for $A_3$ and to $10^{-5}$ M for all other ARs. As a matter of comparison, the native ligand adenosine has an affinity of around $10^{-7}$ M for $A_1$, $A_{2A}$ and $A_3$ and $10^{-6}$ M for $A_{2B}$ (Yan et al., 2003).

More importantly, when SQAd bioconjugate or NPs were preincubated in serum to mimic the *in vivo* conditions, no more binding onto ARs could be detected. This was attributed to the interaction of SQAd with plasma proteins, especially with cholesterol-rich lipoproteins, *i.e.* low-density lipoproteins (LDLs) in humans and high-density lipoproteins in rodents (Sobot et al., 2017b). *In silico* simulations have confirmed that the interaction of the squalene-based bioconjugates with the LDL was driven by the squalene moiety, allowing the hydrophilic adenosine to insert deeply into the LDL hydrophobic core (Yesylevskyy et al., 2018). Thus, LDLs may hinder the possible interaction of SQAd with ARs. As a result, the hypothesis that SQAd may act directly on ARs as a ligand could be rejected.

In order to assess the second hypothesis related to the progressive release of adenosine from SQAd NPs after cell capture, cultured hepatocytes were used. HepG2 cell line was chosen because SQAd NPs concentrated into the liver tissue after intravenous administration (Gaudin et al., 2015).

It was observed that the cell capture of SQAd NPs was independent from the ENTs adenosine transporters. And as ENTs selectively mediate the bidirectional transport of nucleosides, nucleobases and nucleoside analogs (Boswell-Casteel and Hays, 2017), the presence of the

JPET Fast Forward. Published on January 22, 2019 as DOI: 10.1124/jpet.118.254961
This article has not been copyedited and formatted. The final version may differ from this version.



squalene bulky moiety in SQAd was supposed to prevent the interaction of the adenosine fragment with ENTs. By contrast, the cell internalization of SQAd NPs was found to occur through the LDLRs.

As LDLRs are known to trigger the cell internalization via clathrin-dependent endocytosis (Goldstein et al., 1985), it was quite likely that SQAd followed the same pathway, thus ending up in endosomes and then lysosomes. This hypothesis is in perfect agreement with the confocal microscopy images obtained in this study (**Figure 3A**). Once in the lysosomes, SQAd underwent a slow degradation under acidic conditions. Even though cathepsin B alone did not accelerate this proteolytic degradation under tested conditions, its combination with other enzymes like cathepsin D (Couvreur et al., 2006) and proteases may accelerate this phenomenon *in vitro* and *in vivo*. In addition, it was observed that the intracellular cleavage of SQAd into free adenosine resulted also in an extracellular release of adenosine, which gradually increased over time. In other words, SQAd behave as an intracellular reservoir, slowly releasing adenosine in the extracellular medium, probably via ENTs, since these transporters could act bidirectionally. Interestingly, the human brain endothelial hCMEC/D3 cell line showed similar adenosine extracellular release after SQAd NPs internalization which suggests that the interaction of SQAd NPs with HepG2 cells represents a more general trend occurring also in other cell types.

Finally, higher cAMP second messenger levels were observed in cells incubated with the extracellular medium originating from cells treated with SQAd NPs, which clearly indicated an increased activation of ARs. But since adenosine levels in the extracellular medium originating from cells treated with SQAd NPs or free adenosine were very close under the conditions used, adenosine might not be the only factor in the extracellular medium interacting with GPCRs.

In a nutshell, this study led to a better understanding of SQAd NPs mechanism of action as illustrated in **Figure 7**. Unlike currently proposed agonists and antagonists of ARs, SQAd NPs do not interact directly with the ARs but function in a very original way, as a prodrug delivering high quantities of adenosine into the cells. Hence, cells dispose of an important intracellular reservoir of adenosine, progressively releasing the nucleoside which, in turn, can act as an autocrine or paracrine factor. In conclusion, SQAd NPs provide an efficient system for prolonged adenosine delivery resulting in AR activation. This new delivery pathway may open interesting prospects in terms of clinical applications.

## 8. Acknowledgements

Authors would like to thank Ghozlene Mekhloufi and Assia Hessani, Stéphanie Denis, Juliette Vergnaud and Romain Brusini (Institut Galien, France) respectively for experiments involving radioactivity, cell culture experiments, Western blots and flow cytometry; Valérie Nicolas (IPSIT, France) for confocal microscopy; Delphine Courilleau (CIBLOT, IPSIT, France) for experiments on cAMP; Rongfang Liu (Division of Medicinal Chemistry, the Netherlands) for preliminary experiments on radiobinding and cell membrane preparation.

## 9. Authors contributions

Participated in research design: *Rouquette, Lepetre-Mouelhi and Couvreur*

Conducted experiments: *Rouquette, Dufrançais, Yang, Mougin*

Contributed new reagents or analytic tools: *Pieters and Garcia-Argote*

Performed data analysis: *Rouquette*

Wrote or contributed to the writing of the manuscript: *Rouquette, Lepetre-Mouelhi, Yang, IJzerman and Couvreur*

## References

Baldwin SA, Beal PR, Yao SY, King AE, Cass CE and Young JD (2004) The equilibrative nucleoside transporter family, SLC29. *Pflügers Archiv* **447**:735-743.

Borea PA, Gessi S, Merighi S, Vincenzi F and Varani K (2018) Pharmacology of Adenosine Receptors: The State of the Art. *Physiological reviews* **98**:1591-1625.

Boswell-Casteel RC and Hays FA (2017) Equilibrative nucleoside transporters-A review. *Nucleosides, Nucleotides and Nucleic Acids* **36**:7-30.

Cheng Y-C and Prusoff WH (1973) Relationship between the inhibition constant (Ki) and the concentration of inhibitor which causes 50 per cent inhibition (I50) of an enzymatic reaction. *Biochemical pharmacology* **22**:3099-3108.

Couvreur P, Stella B, Reddy LH, Hillaireau H, Dubernet C, Desmaële D, Lepêtre-Mouelhi S, Rocco F, Dereuddre-Bosquet N and Clayette P (2006) Squalenoyl nanomedicines as potential therapeutics. *Nano letters* **6**:2544-2548.

Fredholm BB, IJzerman AP, Jacobson KA, Linden J and Müller CE (2011) International Union of Basic and Clinical Pharmacology. LXXXI. Nomenclature and classification of adenosine receptors—an update. *Pharmacological reviews* **63**:1-34.

Gaudin A, Lepetre-Mouelhi S, Mougin J, Parrod M, Pieters G, Garcia-Argote S, Loreau O, Goncalves J, Chacun H and Courbebaisse Y (2015) Pharmacokinetics, biodistribution and metabolism of squalenoyl adenosine nanoparticles in mice using dual radio-labeling and radio-HPLC analysis. *Journal of Controlled Release* **212**:50-58.

Gaudin A, Yemisci M, Eroglu H, Lepetre-Mouelhi S, Turkoglu OF, Dönmez-Demir B, Caban S, Sargon MF, Garcia-Argote S and Pieters G (2014) Squalenoyl adenosine nanoparticles provide neuroprotection after stroke and spinal cord injury. *Nature nanotechnology* **9**:1054.

Goldstein JL, Brown MS, Anderson RG, Russell DW and Schneider WJ (1985) Receptor-mediated endocytosis: concepts emerging from the LDL receptor system. *Annual review of cell biology* **1**:1-39.

Heitman LH, Goblyos A, Zweemer AM, Bakker R, Mulder-Krieger T, van Veldhoven JP, de Vries H, Brussee J and IJzerman AP (2009) A series of 2, 4-disubstituted quinolines as a new class of allosteric enhancers of the adenosine A3 receptor. *Journal of medicinal chemistry* **52**:926-931.

Reddy LH, Dubernet C, Mouelhi SL, Marque PE, Desmaele D and Couvreur P (2007) A new nanomedicine of gemcitabine displays enhanced anticancer activity in sensitive and resistant leukemia types. *Journal of controlled release* **124**:20-27.

Sobot D, Mura S, Rouquette M, Vukosavljevic B, Cayre F, Buchy E, Pieters G, Garcia-Argote S, Windbergs M and Desmaële D (2017a) Circulating Lipoproteins: A Trojan Horse Guiding Squalenoylated Drugs to LDL-Accumulating Cancer Cells. *Molecular Therapy* **25**:1596-1605.

Sobot D, Mura S, Yesylevskyy SO, Dalbin L, Cayre F, Bort G, Mougin J, Desmaële D, Lepetre-Mouelhi S and Pieters G (2017b) Conjugation of squalene to gemcitabine as unique approach exploiting endogenous lipoproteins for drug delivery. *Nature Communications* **8**:15678.

Yang X, Dong G, Michiels TJ, Lenselink EB, Heitman L, Louvel J and IJzerman AP (2017) A covalent antagonist for the human adenosine A2A receptor. *Purinergic signalling* **13**:191-201.

Yesylevskyy SO, Ramseyer C, Savenko M, Mura S and Couvreur P (2018) Low-Density Lipoproteins and Human Serum Albumin as Carriers of Squalenoylated Drugs: Insights from Molecular Simulations. *Molecular pharmaceutics* **15**:585-591.

## Footnotes

This research project was partly funded by a PhD traineeship grant from the ULLA European University Consortium for Pharmaceutical Sciences.

JPET Fast Forward. Published on January 22, 2019 as DOI: 10.1124/jpet.118.254961
This article has not been copyedited and formatted. The final version may differ from this version.



## Figure legends

**Figure 1** Displacement of specific radioligands binding from the human adenosine receptors $A_1$ (*red circle*), $A_{2A}$ (*orange square*), $A_{2B}$ (*yellow triangle*) and $A_3$ (*green diamond*) by increasing concentrations of squalene-adenosine (SQAd) bioconjugate (**A and C**) or SQAd nanoparticles (NPs) (**B and D**) diluted in assay buffer (**A and B**) or preincubated for 4 h at 37 °C in fetal bovine serum (FBS) (**C and D**). Displacement experiments were performed at 25 °C. TB: total binding; NSB: non-specific binding. Data represent mean values ± standard deviation of three independent experiments.

**Figure 2** Uptake of radiolabeled SQ-[$^3$H]-Ad NPs (*red circle*) or [$^3$H]-adenosine (*orange square*) by HepG2 cells (37 °C over 24 h). Data represent mean values ± standard deviation of two independent experiments.

**Figure 3** Cell uptake of fluorescently labeled SQAd NPs by HepG2 cells. (**A, B**) Confocal microscopy images of HepG2 cells incubated for 2 h with (**A**) fluorescently labeled SQAd NPs or (**B**) the fluorescent tag BODIPY-cholesteryl ester dye as a control, prepared under the same conditions as NPs. Cell membranes were stained with wheat germ agglutinin Alexa Fluor 555 (red) while DAPI was used to visualize nuclei (blue). Scale bar = 10 μm. (**C, D**) Relative fluorescence measured by flow cytometry from HepG2 cells incubated for 30 min or 2 h with fluorescently labeled SQAd NPs. (**C**) Cells treated with NPs were incubated in the absence (*bright red bars*) or in the presence (*dark red bars*) of dipyridamole (dipy). (**D**) Cells were preincubated for 24 h with FBS-supplemented (*bright red bars*) or LPDS-supplemented DMEM (*pink bars*). Cell auto-fluorescence was subtracted from each data set. Data represent mean values ± standard deviation

of three independent experiments. ** indicates $p < 0.01$, two-way ANOVA with Tukey's post hoc test.

**Figure 4** (**A**) Percentage of intact SQAd after incubation until 24 h, with or without cathepsin B (pH 4.8, 37 °C). Data represent mean values ± standard deviation of two independent experiments. (**B**) Representative HPLC chromatogram of partial activation of SQAd into adenosine (Ad) (24 h incubation, pH 4.8, 37 °C, in the presence of cathepsin B). Of note, the peak corresponding to SQAd is not visible in the elution conditions used for adenosine detection.

**Figure 5** Concentrations of adenosine released in the extracellular medium from HepG2 cells exposed to various treatments. (**A**) Cells were incubated for indicated times with 100 µM of SQAd NPs (*red bars*), adenosine (Ad) (*orange bars*) or 5 wt. % dextrose (*yellow bars*) and released adenosine concentrations were measured 1 h following cell culture medium renewal. (**B**) Cells were incubated for 2 h with 100 µM of SQAd NPs (*red circles*), adenosine (Ad) (*orange squares*) or 5 wt. % dextrose (*yellow triangles*) and released adenosine concentrations were measured at different times. Data represent mean values ± standard deviation of three (**A**) or two (**B**) independent experiments.

**Figure 6** Changes in intracellular cAMP levels of naïve cells incubated during 15 min with extracellular medium collected from other cells exposed to SQAd NPs, free adenosine (Ad) or 5 wt. % dextrose (Dext). Changes in relative luminescence units (ΔRLU) were calculated as the difference in light units between treated and untreated cells. Data represent mean values ± standard deviation of three independent experiments. ** indicates $p < 0.01$, one-way ANOVA with Tukey's post hoc test.

**Figure 7** Schema of the interaction of SQAd NPs with cells. (1) The SQAd NPs are taken-up by the cells through the LDL receptors. (2) When located in the intracellular endo-lysosomal compartments, SQAd behaves as an intracellular reservoir, progressively releasing adenosine. (3) Adenosine is finally discharged outside of the cell and (4) interacts with ARs as an autocrine or paracrine signal. Ad: adenosine; AR: adenosine receptor; ENT: equilibrative nucleoside transporter; LDL: low-density lipoproteins; LDLR: LDL receptor; NPs: nanoparticles; SQAd: squalene-adenosine.

JPET Fast Forward. Published on January 22, 2019 as DOI: 10.1124/jpet.118.254961
This article has not been copyedited and formatted. The final version may differ from this version.



# Tables

**Table 1** SQAd bioconjugate and SQAd NPs pKi magnitude for each adenosine receptor.

| | **pKi** | | | |
|---|---|---|---|---|
| | **$A_1$** | **$A_{2A}$** | **$A_{2B}$** | **$A_3$** |
| **SQAd bioconjugate** | ≤ 4 | < 5 | ≤ 4 | < 6 |
| **SQAd NPs** | < 4 | < 4 | < 5 | < 5 |

The pKi values were determined from the radioligand displacement curves using the Cheng-Prusoff equation.

JPET Fast Forward. Published on January 22, 2019 as DOI: 10.1124/jpet.118.254961
This article has not been copyedited and formatted. The final version may differ from this version.

# Figures

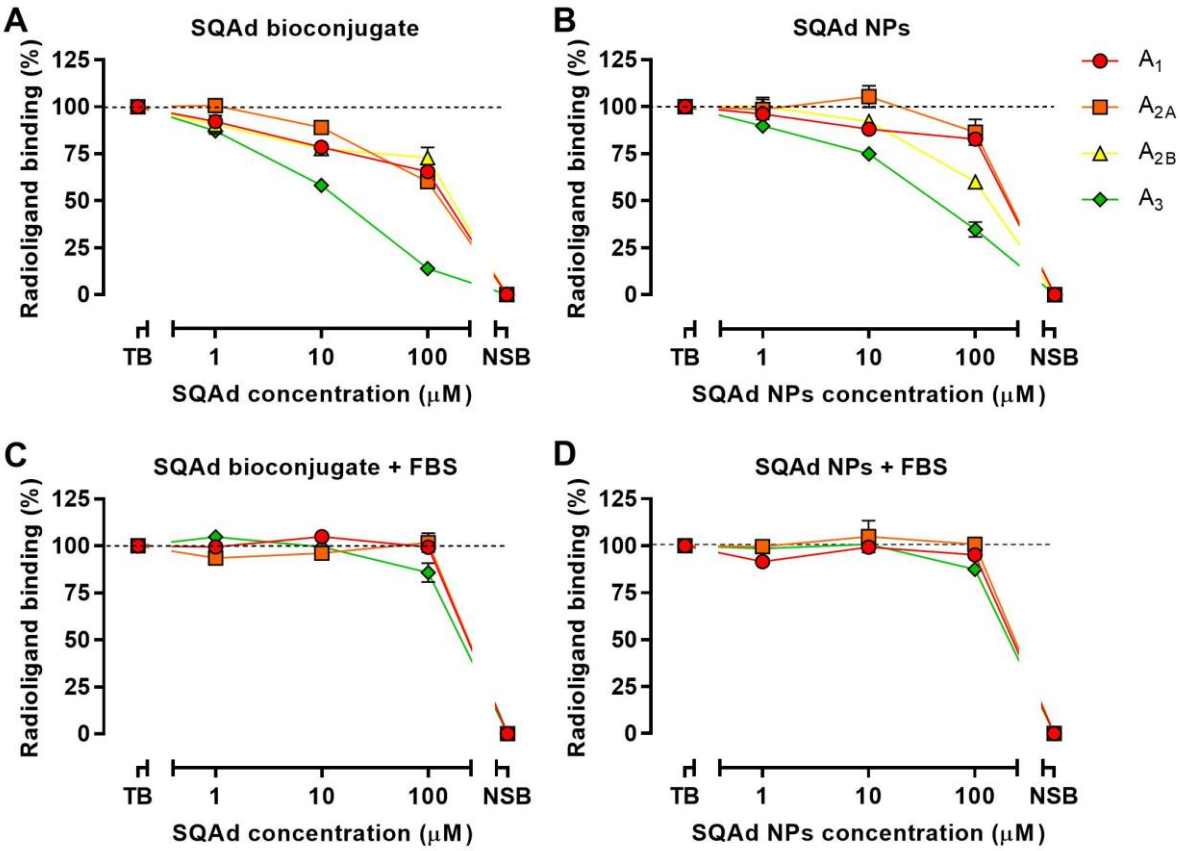


**Figure 1**

JPET Fast Forward. Published on January 22, 2019 as DOI: 10.1124/jpet.118.254961
This article has not been copyedited and formatted. The final version may differ from this version.

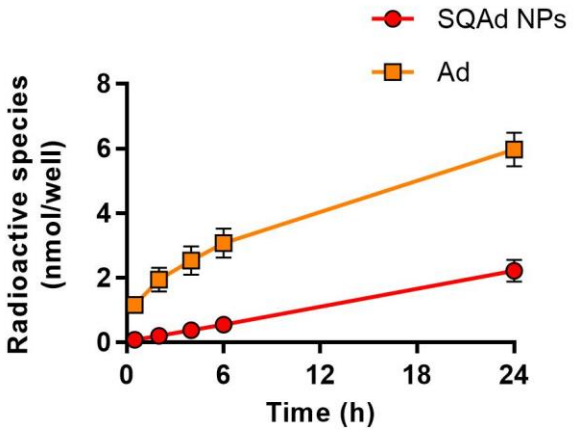


**Figure 2**

JPET Fast Forward. Published on January 22, 2019 as DOI: 10.1124/jpet.118.254961
This article has not been copyedited and formatted. The final version may differ from this version.

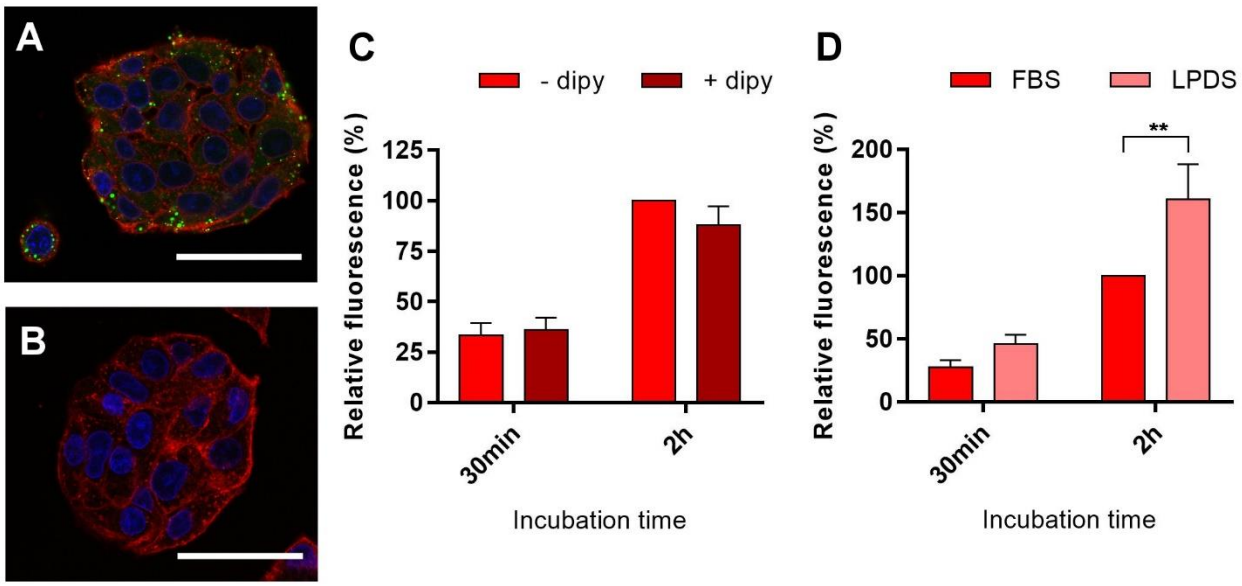


**Figure 3**

JPET Fast Forward. Published on January 22, 2019 as DOI: 10.1124/jpet.118.254961
This article has not been copyedited and formatted. The final version may differ from this version.

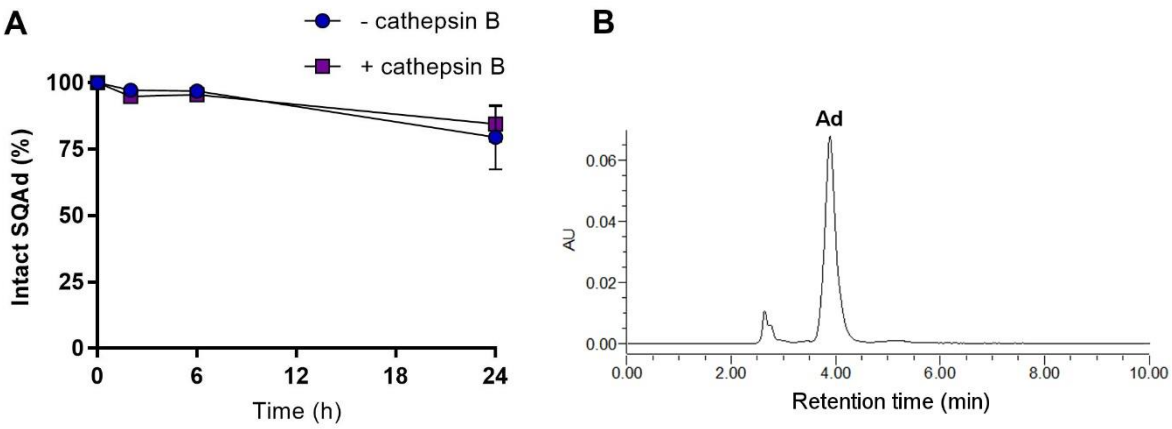


**Figure 4**

JPET Fast Forward. Published on January 22, 2019 as DOI: 10.1124/jpet.118.254961
This article has not been copyedited and formatted. The final version may differ from this version.

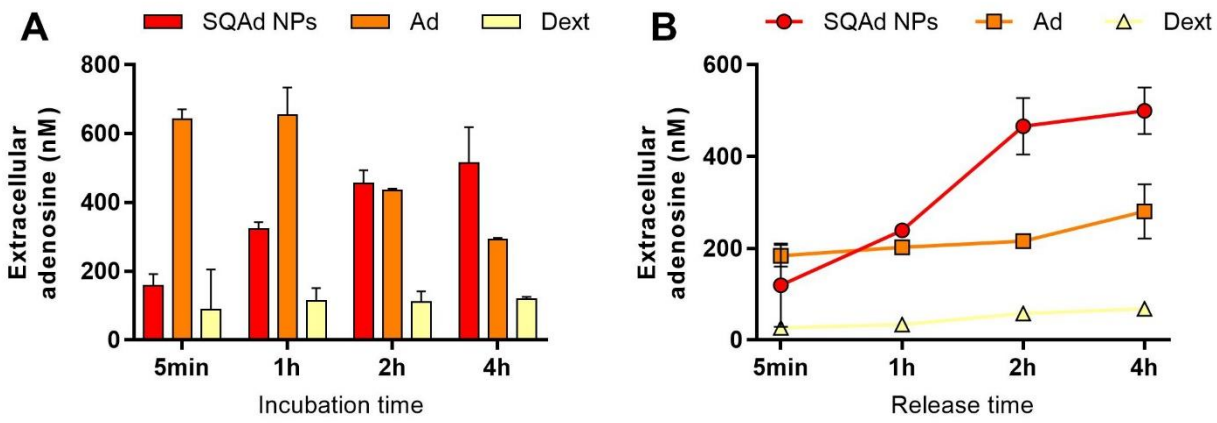


**Figure 5**

JPET Fast Forward. Published on January 22, 2019 as DOI: 10.1124/jpet.118.254961
This article has not been copyedited and formatted. The final version may differ from this version.

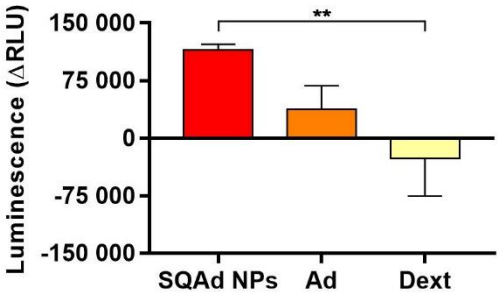


**Figure 6**

JPET Fast Forward. Published on January 22, 2019 as DOI: 10.1124/jpet.118.254961
This article has not been copyedited and formatted. The final version may differ from this version.

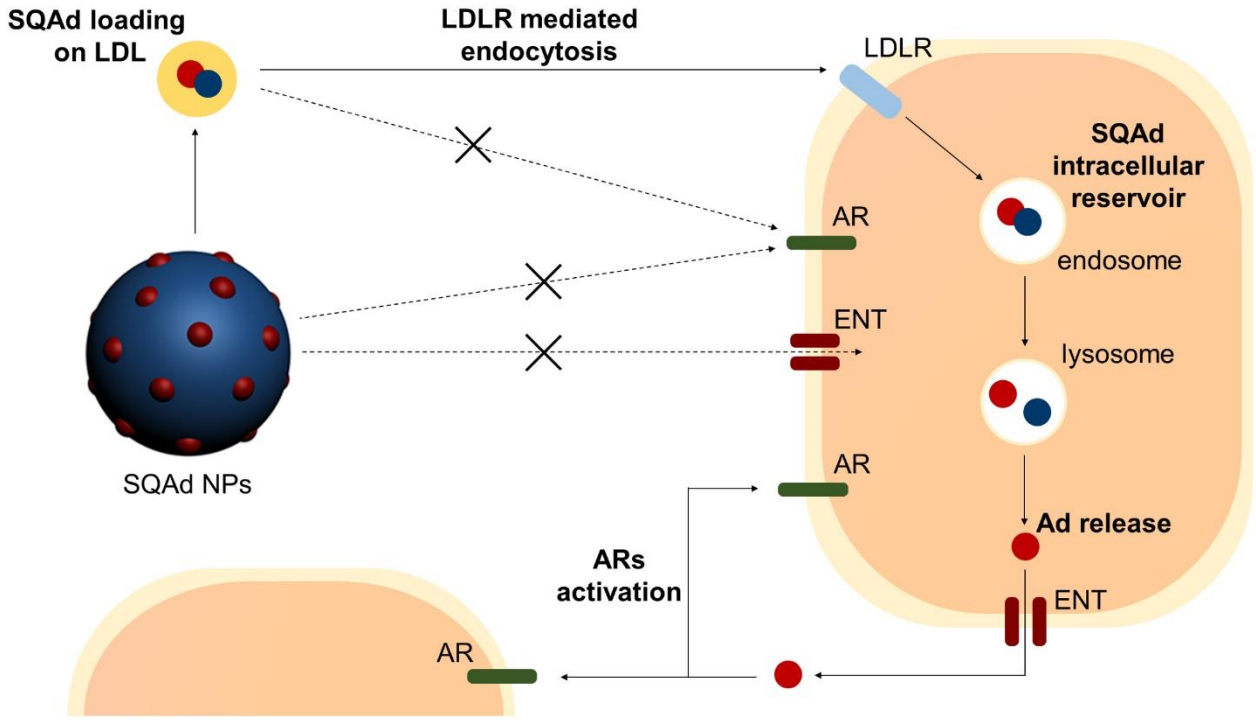


**Figure 7**